Electronic Supplementary Material (ESI) for Chemical Communications
This journal is © The Royal Society of Chemistry 2013

Supporting Information

Pillar substitution modulates CO_2 affinity in "mmo" topology networks

Mona H. Mohamed,[a, b,]†Sameh K. Elsaidi,[a, b,]† Tony Pham,[a] Katherine A. Forrest,[a]Brant Tudor,[a] Lukasz Wojtas,[a] Brian Space[a] and Michael J. Zaworotko[a]

Department of Chemistry, CHE205, University of South Florida, 4202 E. Fowler Avenue, Tampa, FL, 33620, USA

[‡]Chemistry Department, Faculty Of Science, Alexandria University, P.O.Box 426 Ibrahimia, Alexandria 21321, Egypt

Experimental procedures:

Materials and Methods: All reagents and solvents were purchased in high purity grade and used as received. Powder X-ray diffraction (PXRD) data were recorded on a BrukerD8 Advance X-ray diffractometer at 20 kV, 5 mA for Cukα (λ = 1.5418 Å), with a scan speed of 0.5 s/step (6°/min) and a step size of 0.05° in 2θ at room temperature. The calculated XPD patterns were generated using Powder Cell for Windows Version 2.4 (programmed by W. Kraus and G. Nolze, BAM Berlin, 2000). Infrared spectra were recorded on a Nicolet Avatar 320 FT-IR spectrometer. Low pressure gas adsorption isotherms were measured on the Micromeritics ASAP 2020 Surface Area and Porosity Analyzer**.**

Synthesis:

[Ni(bpe)$_2$WO$_4$], WOFOUR-1-Ni (1)

An aqueous solution (4mL) of $NiCl_2.6H_2O$ (11.9 mg, 0.05 mmol) was mixed with an aqueous solution (4mL) of $Na_2WO_4.2H_2O$ (16.5 mg, 0.05mmol) in a long thin test tube, the resulting turbid solution was carefully layered under1,2-bis(4-pyridyl)ethene (bpe) (18.2 mg, 0.1 mmol) in 4 mL of acetonitrile and water (v/v = 2:1). The tube was sealed and left undisturbed at room temperature. After one weeklight green block-shaped crystals were isolated.

[Co(bpe)$_2$WO$_4$], WOFOUR-1-Co (2)

Crystals of **2** were prepared in the same way as **1** except that $CoCl_2.6H_2O$ (11.9 mg, 0.05mmol) was used instead of $NiCl_2.6H_2O$. After one week, the red block-shaped crystals were harvested.

Scheme 1. Pillar substitution in **mmo** nets has little effect upon structure in CROFOUR-1-Ni, MOOFOUR-1-Ni and WOFOUR-1-Ni.

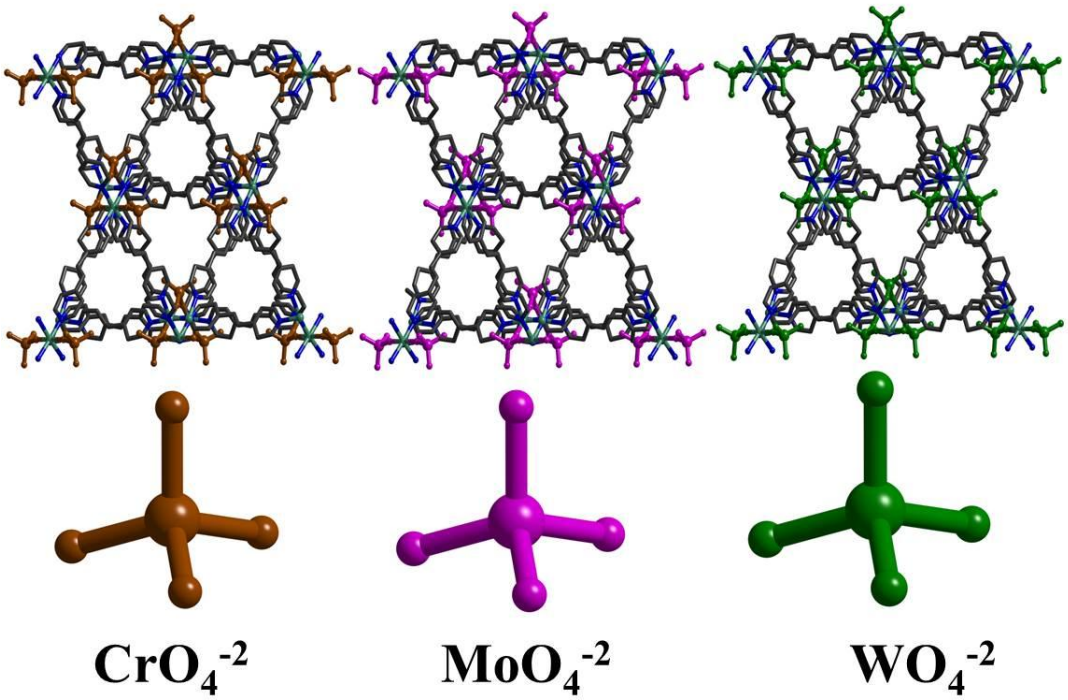

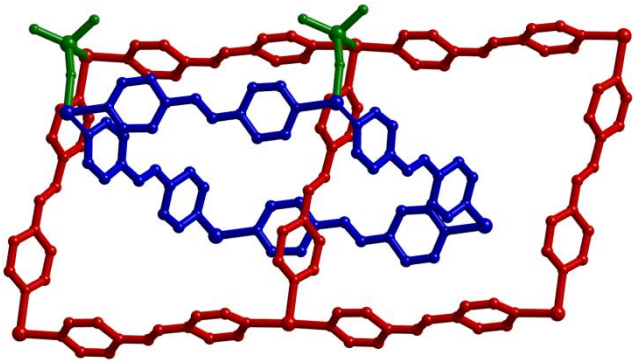

Figure S1. Self-catenated square grids (red and blue) connected with WO_4^{-2} pillars (green) to afford **mmo** net.

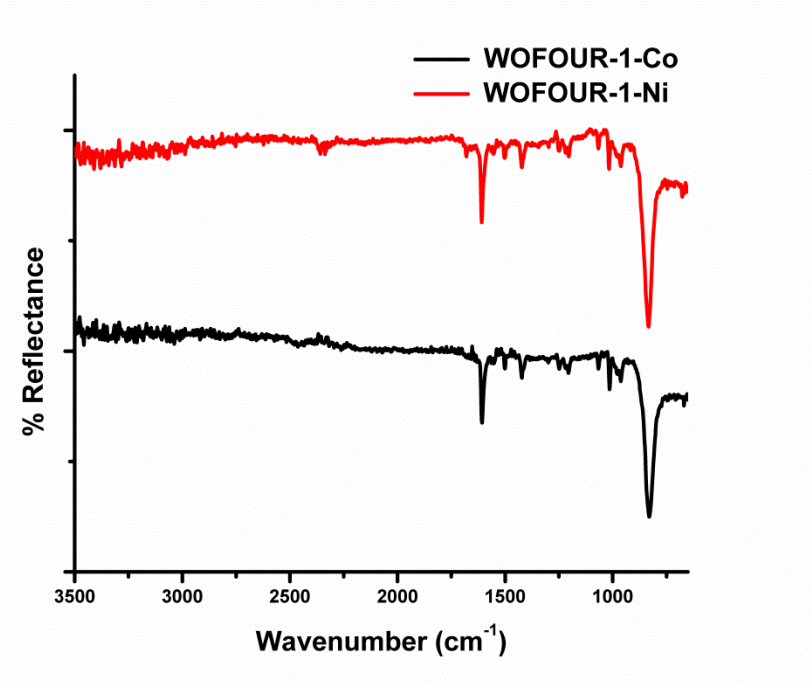

Figure S2. Infrared spectroscopy (diffuse reflectance) for WOFOUR-1-Co and WOFOUR-1-Ni.

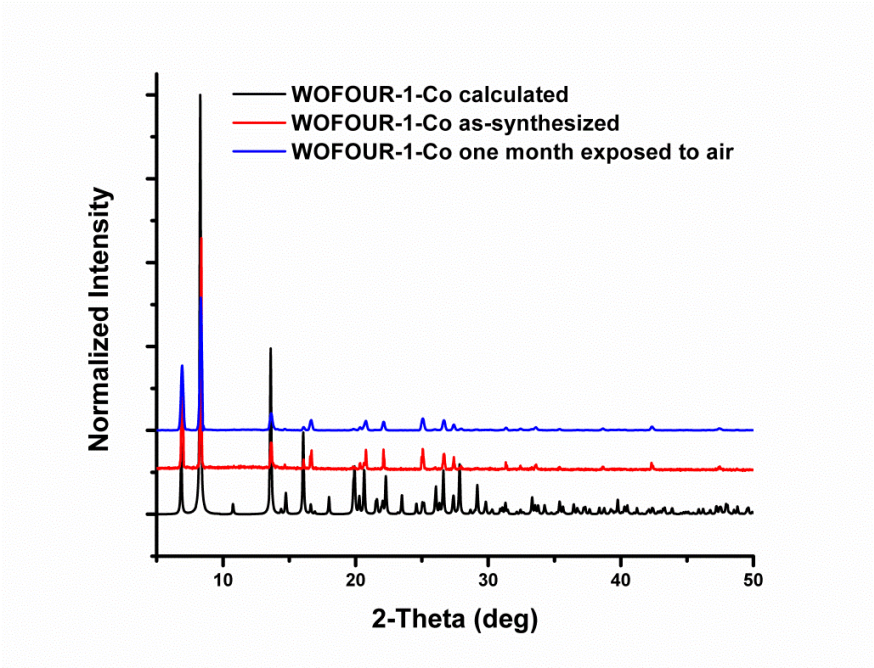

Figure S3. Calculated and experimental (as-synthesized and air exposed sample)Powder X-ray diffraction(PXRD) patterns for WOFOUR-1-Co.

Stability of WOFOUR-1-Ni

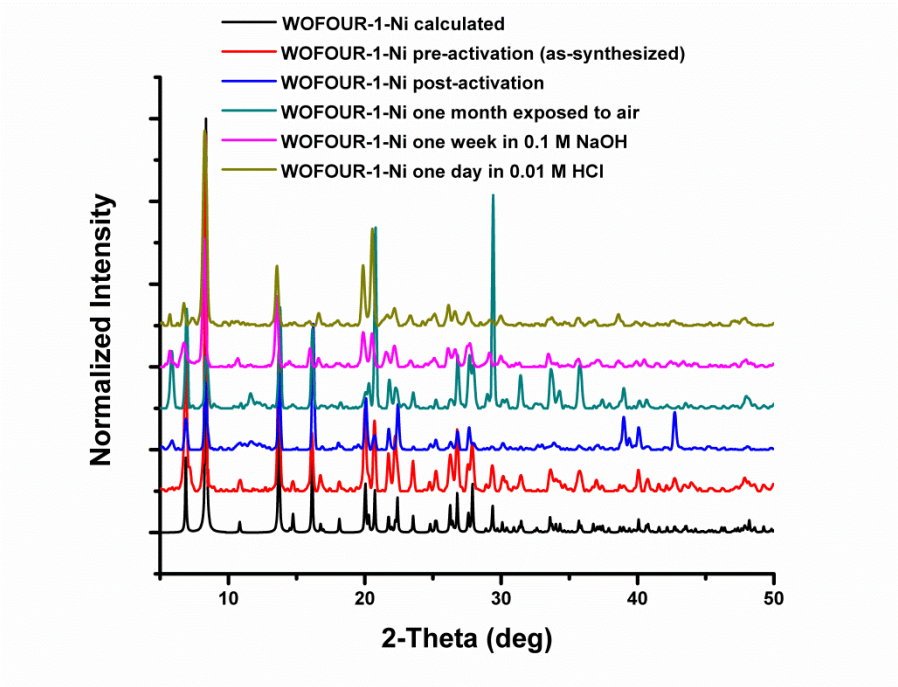

Figure S4.PXRD patterns for WOFOUR-1-Ni addressing itsstability after activation, in water in air, in 0.1 M NaOH and in 0.01M HCl.

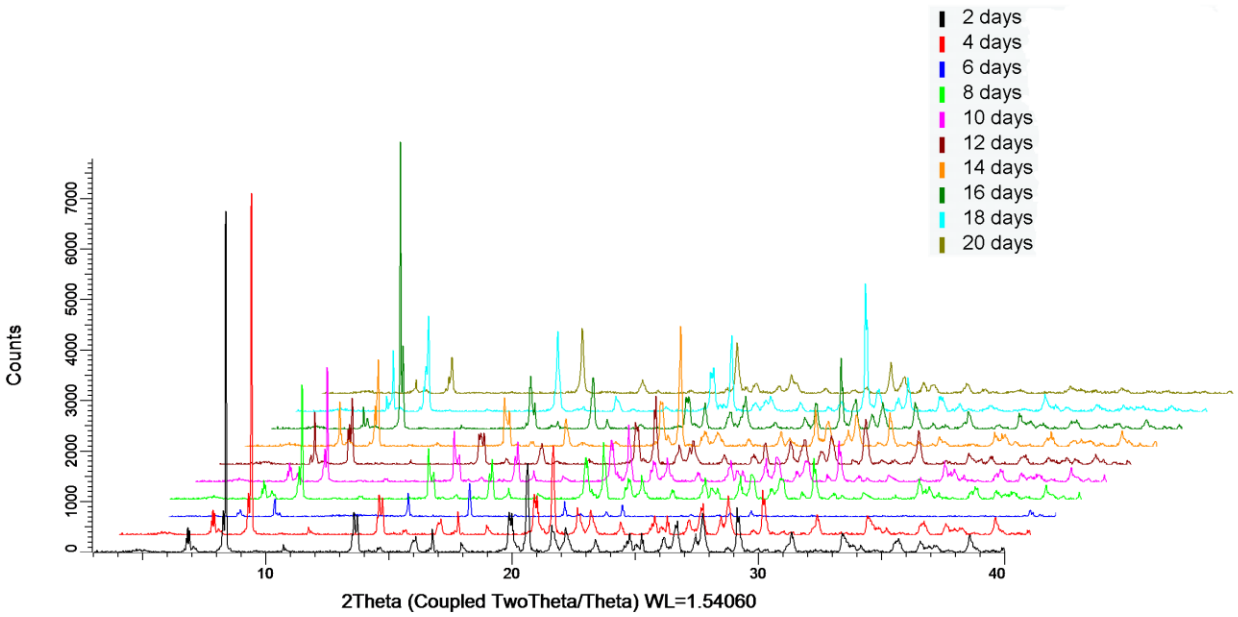

Figure S5.PXRD patterns for WOFOUR-1-Ni addressing its stability in boiling water for up to 20 days.

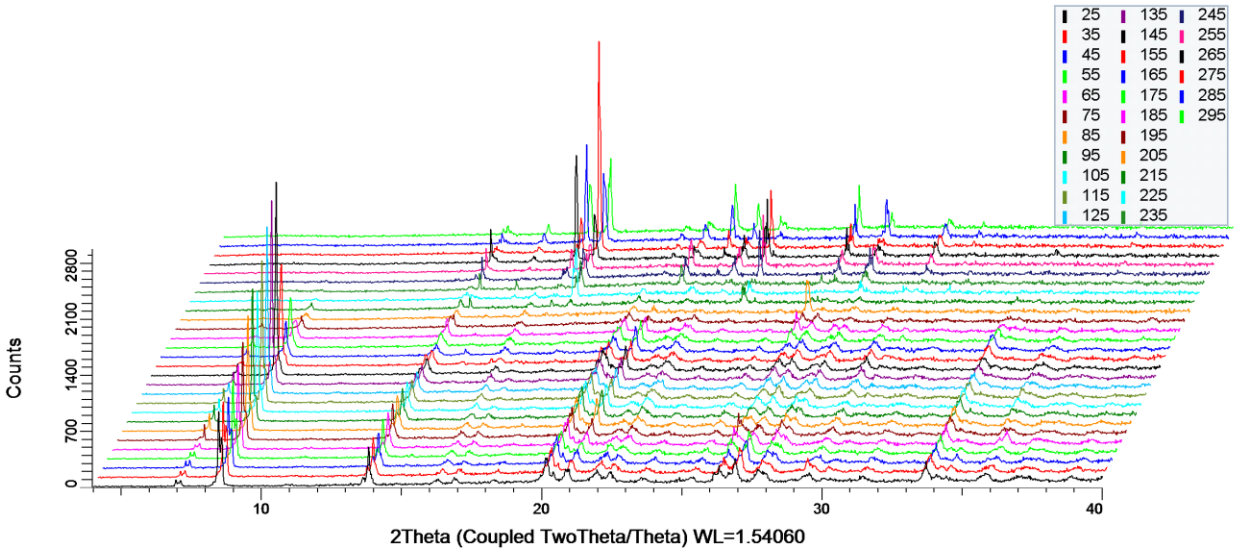

Figure S6. Variable temperature PXRD patterns for WOFOUR-1-Ni addressing its thermal stability.

Gas sorption properties:

$[Ni(bpe)_2WO_4]$, WOFOUR-1-Ni activation for gas sorption

The as-synthesized crystals of WOFOUR-1-Ni were exchanged with acetonitrile for 48 h (2 times/day) then the crystals in acetonitrile are heated up in the ovenat 80°C for 3h. The resulting solid was filtered, evacuated at 60°Cfor 12 h and then at 80°C for 4 h under dynamic pressure. Due to the strong interaction between CO_2 and the frameworkwhich is accompanied by slow CO_2 sorption kinetics, we had increased the equilibrium time during the CO_2 adsorption measurement.

Table S1: Gas Adsorption Properties of CROFOUR-1-Ni, MOOFOUR-1-Ni, WOFOUR-1-Ni.

MOM	**CROFOUR-1-Ni**	**MOOFOUR-1-Ni**	**WOFOUR-1-Ni**
Empirical Formula	$[Ni(bpe)_2CrO_4]$	$[Ni(bpe)_2MoO_4]$	$[Ni(bpe)_2WO_4]$
Langmuir Surface Area (m^2/g)	505	456	315
CO_2 Uptake (1 atm, 298 K; cm^3/g)	43	55	52
CO_2 Uptake (1 atm, 298 K; cm^3/cm^3)	52	69	76
CO_2 Uptake (0.15 atm, 298 K; cm^3/g)	23	27	22
CO_2 Uptake (0.15 atm, 298 K; cm^3/cm^3)	28	33	33
CO_2Q_{st} (zero loading; kJ/mol)	50	56	66
CO_2/CH_4selectivity (50/50; Zero loading, 298 K)	170	182	372
CO_2/CH_4 selectivity (50/50; 1 atm, 298 K)	25	40	26
CO_2/N_2 selectivity (10/90; Zero loading, 298 K)	1240	1820	2158
CO_2/N_2 selectivity (10/90; 1 atm, 298 K)	195	96	179

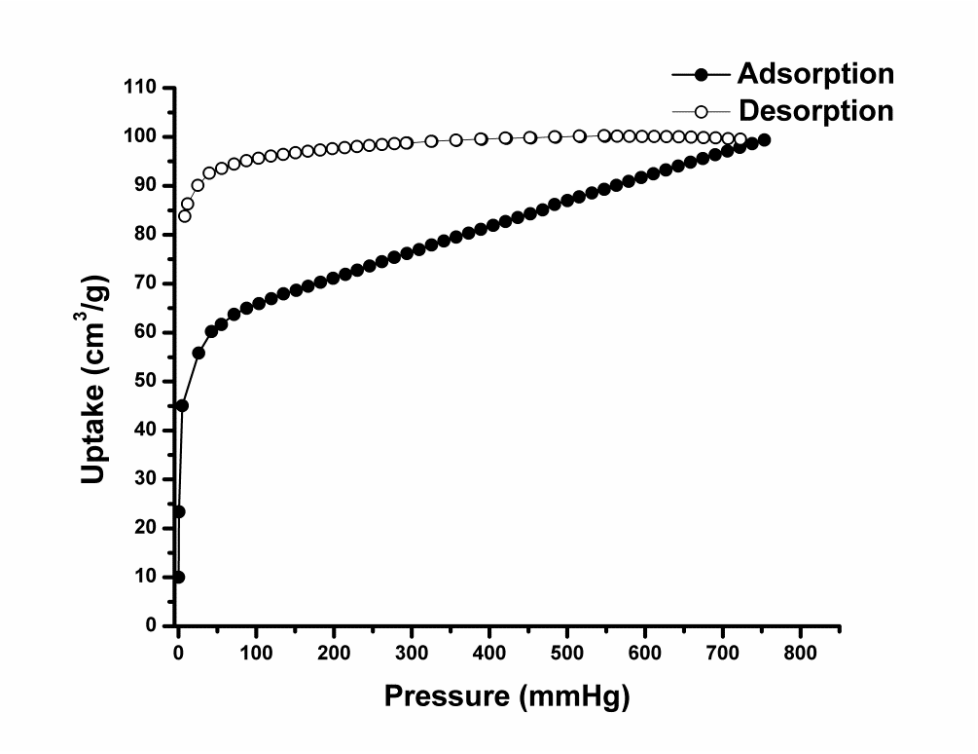

Figure S7. CO_2 isotherm of WOFOUR-1-Ni measured at 195 K.

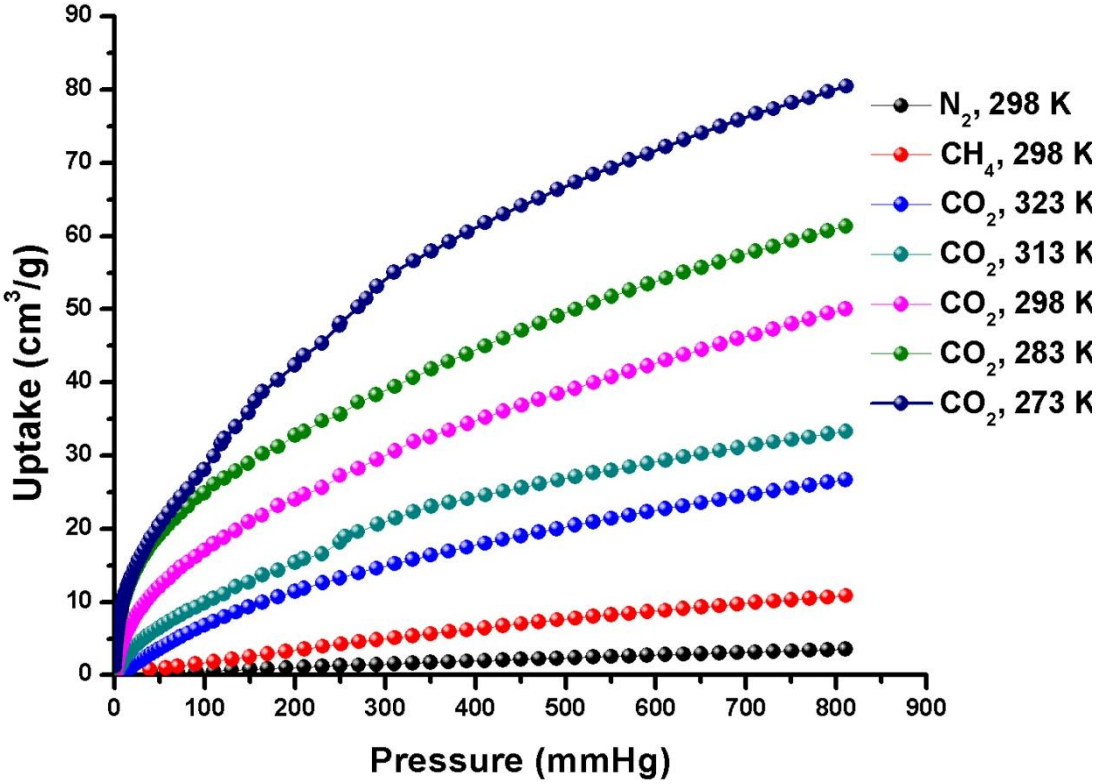

Figure S8. Reversible single component gas adsorption isotherms of WOFOUR-1-Ni.

Calculation of isosteric heat of adsorption(Q_{st}):

The Q_{st}values for WOFOUR-1-Ni have been calculated according to virial equation using the fitted adsorption isotherms at 273 K and 298 K correspondingly it has been calculated using the fitting of the adsorption isotherms at five different temperatures; 273 K, 283 K, 298 K, 313 K and 323 K.

Table S2: isosteric heat of adsorption (Q_{st}) of CO_2 at zero coverage in metal organic materials that showed high CO_2 affinity.

MOM	**Isosteric heat of adsorption (-Q_{st}) (kJ/mol)**	**Reference**
CD-MOF-2	113.5	1
Cu-BTTri-mmen	96	2
Cu-BTTri-en	90	3
Zn(DCTP)(DABCO)	77	4
mmen-Mg_2(dobpdc)	71	5
WOFOUR-1-Ni	65.5	This work
MIL-100(Cr)	62	6
$[(CH_3)_2NH_2]_2[Tb_6(\mu 3\text{-}OH)_8(FTZB)_6(H2O)_6]\cdot(H_2O)_{22}$	58.1	7
MOOFOUR-1-Ni	56	8
NH_2-MIL-53(Al), USO-1-Al-A	50	9
CROFOUR-1-Ni	50	8
CuTATB-30	48	10
CAU-1	48	11
Mg-MOF-74, CPO-27-Mg	47	12
bio-MOF-11	45	13
CuBDPMe	45	14
MIL-101(Cr)	44	6
Ni-MOF-74, CPO-27-Ni	42	15
$Zn_2(ox)(atz)_2$	41	16
$Pd(\mu\text{-}F\text{-}pymo\text{-}N^1,N^3)_2$	40	17
SIFSIX-3-Zn	40	18

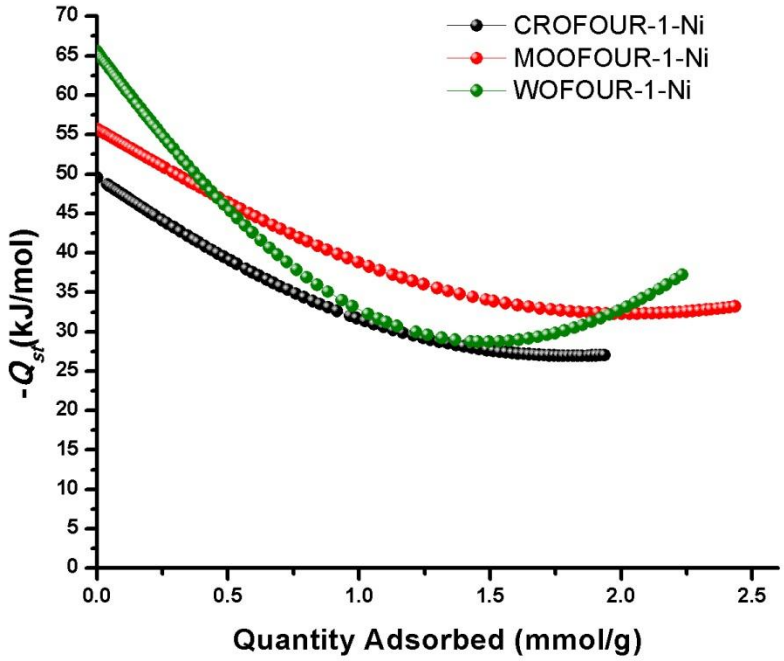

Figure S9. CO_2 isosteric heat of adsorption (Q_{st}) for CROFOUR-1-Ni, MOOFOUR-1-Ni and WOFOUR-1-Ni.

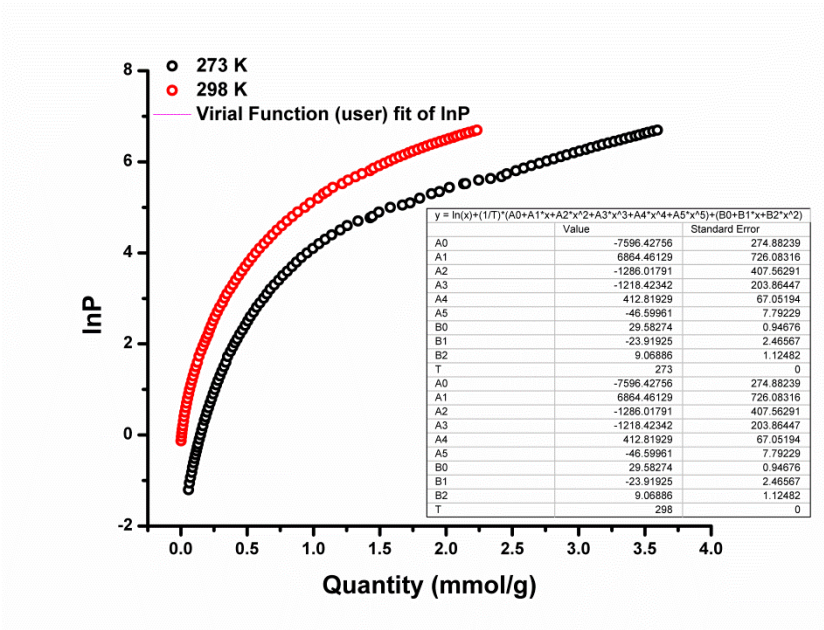

Figure S10. CO_2 adsorption isotherms of WOFOUR-1-Ni at 273 K and 298 K fitted using the virial equation.

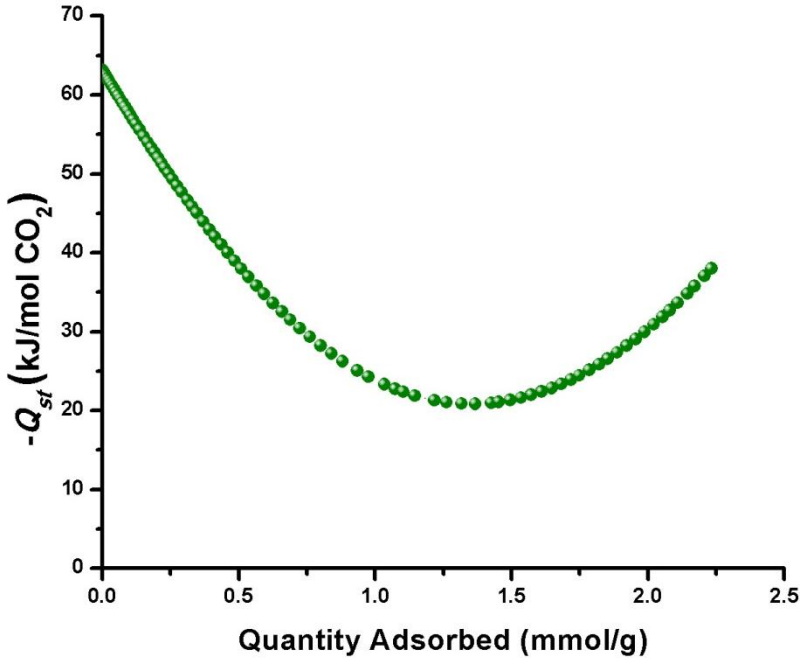

Figure S11. CO_2isosteric heat of adsorption (Q_{st}) for WOFOUR-1-Ni using the fitted data measured at 298 K and 273 K.

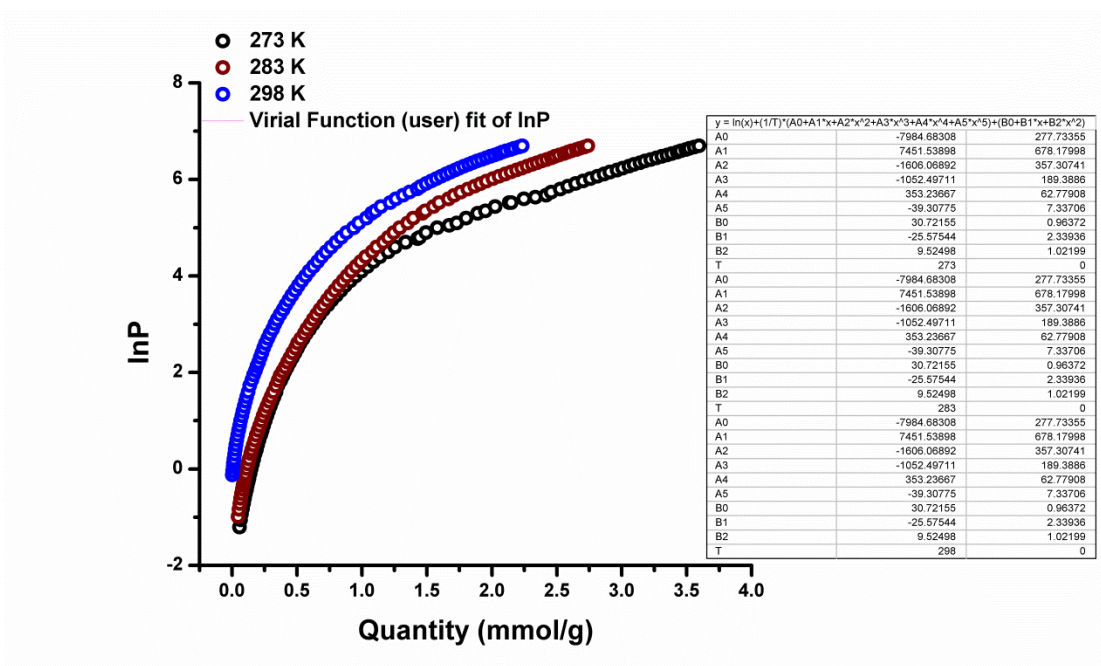

y = ln(x)+(1/T)*(A0+A1*x+A2*x^2+A3*x^3+A4*x^4+A5*x^5)+(B0+B1*x+B2*x^2)		
A0	-7984.68308	277.73355
A1	7451.53898	678.17998
A2	-1606.06892	357.30741
A3	-1052.49711	189.3886
A4	353.23667	62.77908
A5	-39.30775	7.33706
B0	30.72155	0.96372
B1	-25.57544	2.33936
B2	9.52498	1.02199
T	273	0
A0	-7984.68308	277.73355
A1	7451.53898	678.17998
A2	-1606.06892	357.30741
A3	-1052.49711	189.3886
A4	353.23667	62.77908
A5	-39.30775	7.33706
B0	30.72155	0.96372
B1	-25.57544	2.33936
B2	9.52498	1.02199
T	283	0
A0	-7984.68308	277.73355
A1	7451.53898	678.17998
A2	-1606.06892	357.30741
A3	-1052.49711	189.3886
A4	353.23667	62.77908
A5	-39.30775	7.33706
B0	30.72155	0.96372
B1	-25.57544	2.33936
B2	9.52498	1.02199
T	298	0

Figure S12.CO_2 adsorption isotherms of WOFOUR-1-Ni at 273 K, 283 K and 298 K fitted using the virial equation.

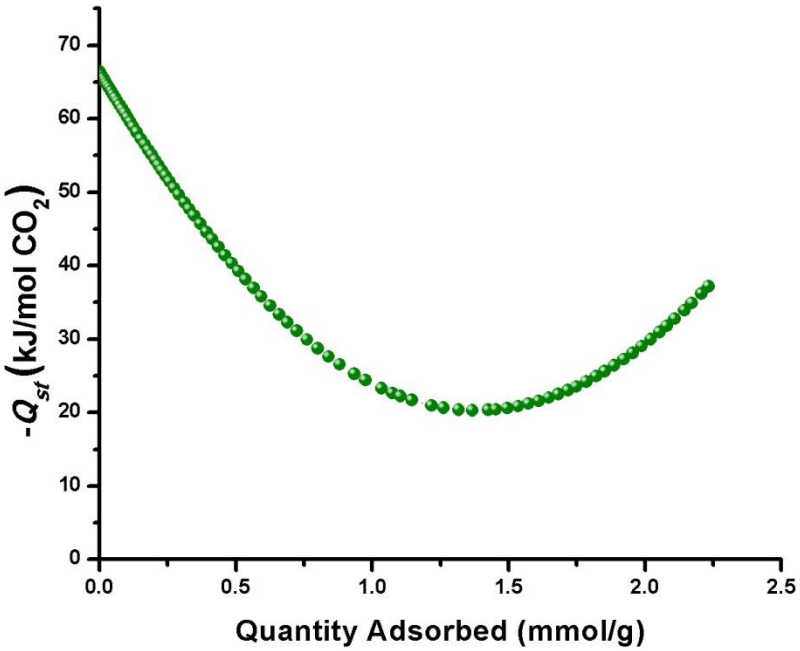

Figure S13. CO_2isosteric heat of adsorption (Q_{st}) for WOFOUR-1-Ni using the fitted data measured at 298 K, 283 K and 273 K.

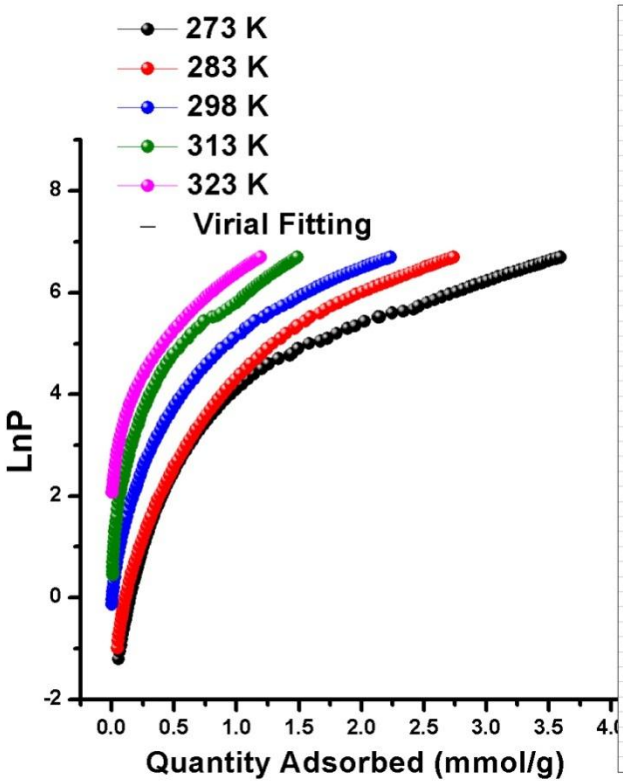

y = ln(x)+(1/T)*(A0+A1*x+A2*x^2+A3*x^3+A4*x^4+A5*x^5)+(B0+B1*x+B2*x^2)		
A0	-7881.45256	135.60828
A1	5341.23908	368.76642
A2	-616.13512	251.03365
A3	-1128.21818	151.03995
A4	383.03766	51.50604
A5	-43.4217	6.15858
B0	30.33576	0.44738
B1	-18.10181	1.19721
B2	6.24985	0.62996
T	273	0
A0	-7881.45256	135.60828
A1	5341.23908	368.76642
A2	-616.13512	251.03365
A3	-1128.21818	151.03995
A4	383.03766	51.50604
A5	-43.4217	6.15858
B0	30.33576	0.44738
B1	-18.10181	1.19721
B2	6.24985	0.62996
T	283	0
A0	-7881.45256	135.60828
A1	5341.23908	368.76642
A2	-616.13512	251.03365
A3	-1128.21818	151.03995
A4	383.03766	51.50604
A5	-43.4217	6.15858
B0	30.33576	0.44738
B1	-18.10181	1.19721
B2	6.24985	0.62996
T	298	0
A0	-7881.45256	135.60828
A1	5341.23908	368.76642
A2	-616.13512	251.03365
A3	-1128.21818	151.03995
A4	383.03766	51.50604
A5	-43.4217	6.15858
B0	30.33576	0.44738
B1	-18.10181	1.19721
B2	6.24985	0.62996
T	313	0
A0	-7881.45256	135.60828
A1	5341.23908	368.76642
A2	-616.13512	251.03365
A3	-1128.21818	151.03995
A4	383.03766	51.50604
A5	-43.4217	6.15858
B0	30.33576	0.44738
B1	-18.10181	1.19721
B2	6.24985	0.62996
T	323	0

Figure S14. CO_2 adsorption isotherms of WOFOUR-1-Ni at 273 K, 283 K, 298 K, 313 K and 323 K fitted using the virial equation.

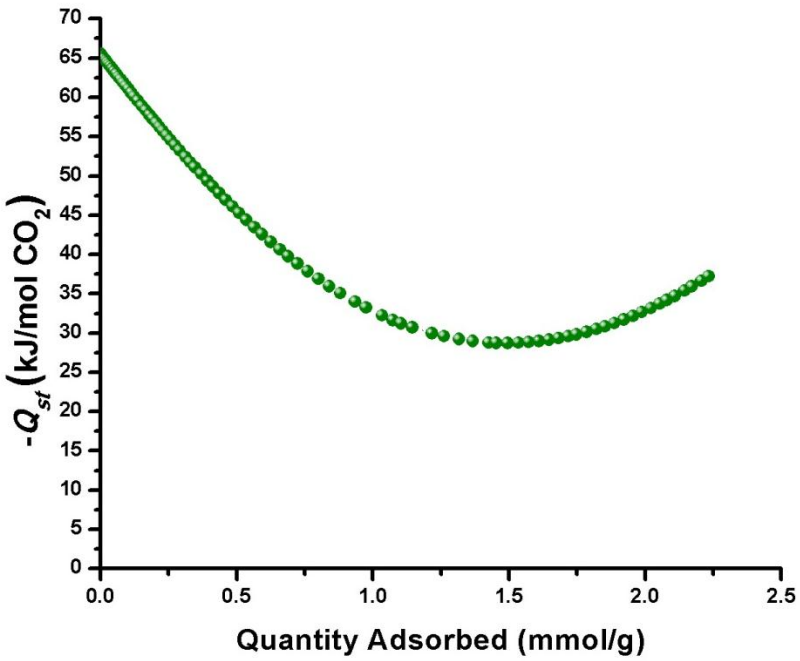

Figure S15. CO_2isosteric heat of adsorption (Q_{st}) for WOFOUR-1-Ni using the fitted data measured at 273 K, 283 K, 298 K, 313 K and 323 K.

Ideal Adsorbed Solution Theory

Ideal adsorbed solution theory, developed by Myers and Prausnitz,[19] was used to estimate the selectivities of CO_2/N_2 (10:90) and CO_2/CH_4 (50:50) mixture compositions in WOFOUR-1-Ni from their respective single-component isotherms. The isotherms were fitted to the dual-site Langmuir-Freundlich equation:[20]

$$n = \frac{n_{m1} b_1 P^{\left(\frac{1}{t_1}\right)}}{1 + b_1 P^{\left(\frac{1}{t_1}\right)}} + \frac{n_{m2} b_2 P^{\left(\frac{1}{t_2}\right)}}{1 + b_2 P^{\left(\frac{1}{t_2}\right)}}$$

Here, n is the amount adsorbed per mass of adsorbent (in mol/kg), P is the total pressure (in kPa) of the bulk gas at equilibrium with the adsorbed phase, n_{m1} and n_{m2} are the saturation uptakes (in mol/kg) for sites 1 and 2, b_1 and b_2 are the affinity coefficients (in kPa^{-1}) for sites 1 and 2, and t_1 and t_2 represent the deviations from the ideal homogeneous surface for sites 1 and 2. The

parameters that were obtained from the fitting for both MOFs are found in Table S3. All isotherms were fitted with $R^2 > 0.9999$.

The fitted parameters were then used to predict multi-component adsorption. The mole fraction of each species in the adsorbed phase can be calculated by solving the expression:

$$\int_0^{\frac{Py_i}{x_i}} \frac{n_i(P)}{P} dP = \int_0^{\frac{Py_j}{x_j}} \frac{n_j(P)}{P} dP$$

where x_i and y_i are the adsorbed and bulk phase mole fractions of component i, respectively. In order to solve for x_i, two quantities must be specified, specifically P and y_i. The quantity x_i was determined using numerical analysis and root exploration. The selectivity for component i relative to component j can be calculated *via* the following:

$$S_{i/j} = \frac{x_i}{x_j}\frac{y_j}{y_i}$$

Table S3: The fitted parameters for the dual-site Langmuir-Freundlich equation for the single-component isotherms of CO_2, N_2, and CH_4 in WOFOUR-1-Ni at 298 K.

	CO_2	**N_2**	**CH_4**
n_{m1} (mol/kg)	6.899934	1.605053	7.364427347
n_{m2} (mol/kg)	0.0540638	0.251865	0.18746686
b_1 (kPa^{-1})	0.0378033	0.001060	0.000944312
b_2 (kPa^{-1})	3.21E-07	0.002424	0.001032247
t_1	1.880802	1.105355	1.18758788
t_2	0.183781	1.025056	0.582959992

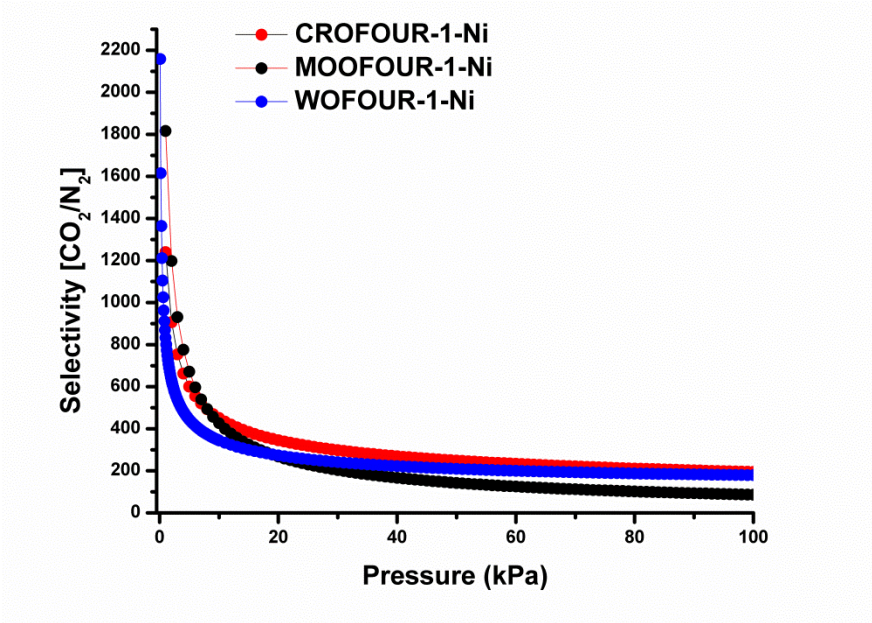

Figure S16.IAST calculated selectivity for a 10:90 CO_2: N_2 mixture based upon experimentally observed adsorption isotherms of the pure gases for WOFOUR-1-Ni.

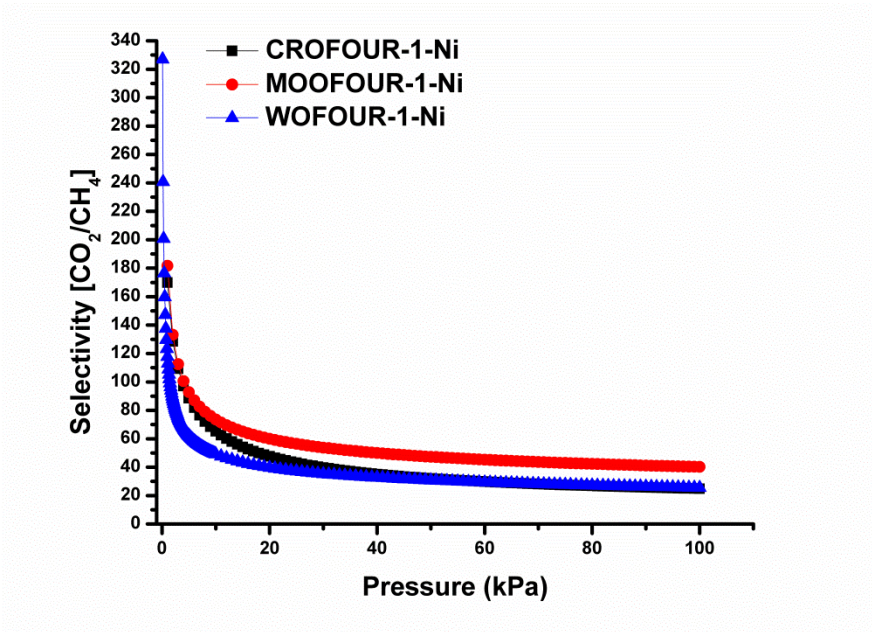

Figure S17.IAST calculated selectivity fora 50:50 CO_2: CH_4mixture based upon the experimentally observed adsorption isotherms of the pure gases for WOFOUR-1-Ni.

Gravimetric selectivity

The wt% of CO_2 at 0.15 bar in WOFOUR-1-Ni was observed to be 4.3 % whereas for N_2 at 0.75 bar value it was found to be 0.31 % affording a selectivity of CO_2 over N_2 under these conditions[21] of 69.

Electronic Structure Calculations and computational study

Electronic structure calculations were performed on CROFOUR-1-Ni, MOOFOUR-1-Ni, and WOFOUR-1-Ni to determine the electrostatic nature of the atoms within the respective MOMs. Examination of the unit cell for all three MOMs revealed 28 atoms in chemically distinct environments (Figure S18). A series of fragments were taken from the crystal structure of the MOMs and charge-fitting calculations were performed on each fragment. The addition of hydrogen atoms, where appropriate, was required for the chemical termination of fragment boundaries. Representational fragments for WOFOUR-1-Ni can be found as XYZ files in the compressed folder for this Communication. Note, fragments of similar type were also chosen for CROFOUR-1-Ni and MOFOUR-1-Ni.

All calculations on each fragment were performed using the NWChem*ab initio* simulation software.[22]All C, H, N, and O atoms were treated with the 6-31G* basis set. For the Ni^{2+}, Cr^{6+}, Mo^{6+}, and W^{6+} ions, the LANL2DZ[23-25]effective core potential basis set was used to treat the inner electrons of these many-electron species. The partial charges were determined through a least-squared fit approach[26,27]to the electrostatic potential surface of each fragment. For each chemically distinct atom, the partial charges were averaged between the fragments. Atoms that are buried or located on the edges of the fragments were not included in the averaging. The averaged partial charges for each chemically distinct atom for all three MOMs can be found in Table S3.The partial charges that were obtained for CROFOUR-1-Ni, MOOFOUR-1-Ni, and WOFOUR-1-Ni were used for the molecular simulation of CO_2 adsorption within the respective compounds in this work. Indeed, electronic structure calculations on all three variants revealed that the partial charges (derived from the electrostatic surface potential) on the terminal oxygen atoms for WOFOUR-1-Ni, MOOFOUR-1-Ni, and CROFOUR-1-Ni are approximately −0.80 e^-, −0.70 e^-, and −0.60 e^-, respectively.

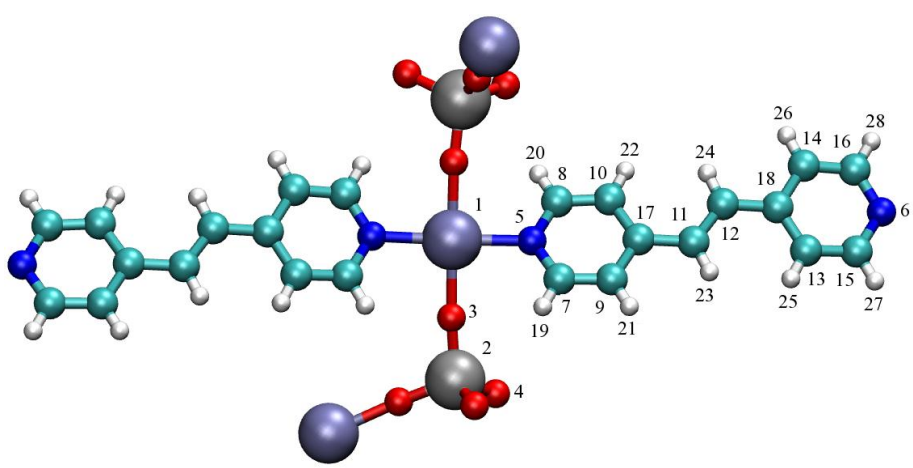

Figure S18. The chemically distinct atoms in $Ni(bpe)_2MO_4$ (M = Cr, Mo, W) defining the numbering system corresponding to Table S3. Atom colors: C = cyan, H = white, N = blue, O = red, Ni = purple, Cr/Mo/W = silver.

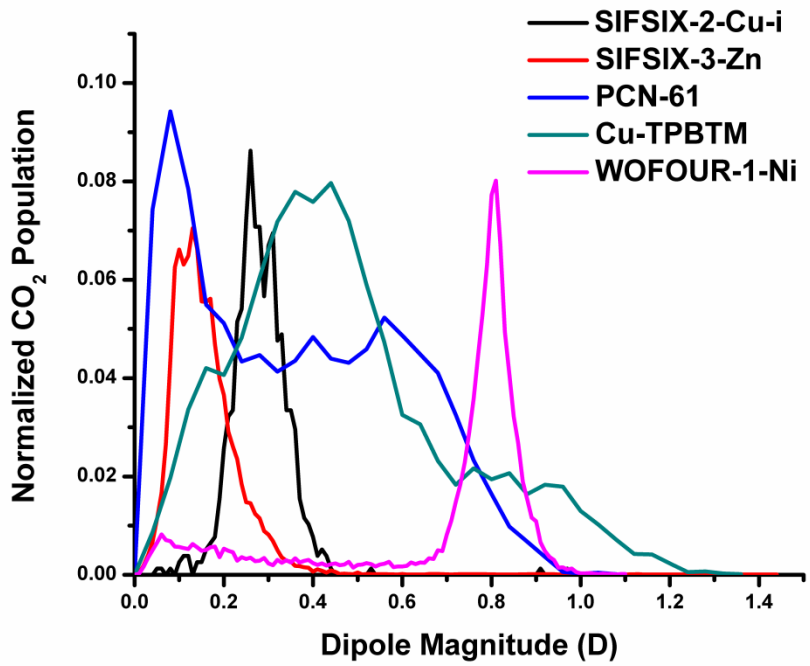

Figure S19. Normalized CO_2 dipole distribution in WOFOUR-1-Ni compared to some selected MOMs that showed high CO_2 affinity, at 298 K and o.1 atm produced from the simulation.

The magnitudes of the induced dipoles on the CO_2 molecules in WOFOUR-1-Ni were compared to those that were produced from the simulations in other MOMs that show strong CO_2 affinity, such as pillared square grids[18] and *rht*-MOFs.[28-31]Specifically, the dipole distributions for WOFOUR-1-Ni were compared to those for SIFSIX-2-Cu-i,[18] SIFSIX-3-Zn,[18,32] PCN-61,[29,30]and Cu-TPBTM[31](Figure S19). Simulations of CO_2 sorption were performed in these MOMs using the force field parameters that were derived for the respective compounds as determined in previous work.[18,33-35]

For SIFSIX-2-Cu-i and SIFSIX-3-Zn, a single peak can be observed from 0.20 to 0.40 D and 0.05 to 0.25 D, respectively. This peak for the respective MOMs corresponds to direct sorption onto the equatorial fluorine atoms in these compounds. Although a high occupancy of CO_2 molecules can be found in this region for these MOMs, the induced dipole magnitudes are not as high as those produced by the primary sorption site in WOFOUR-1-Ni. In PCN-61 and Cu-TPBTM, the peak that corresponds to sorption onto the copper paddlewheel clusters can be seen in the range 0.5 to 0.95 D and 0.70 to 1.2 D, respectively. Note, the other peaks in the CO_2 dipole distribution for PCN-61 and Cu-TPBTM correlate to other sorption sites inside these *rht*-MOFs. The unsaturated Cu^{2+} ions can cause the CO_2 molecules to exhibit a high dipole magnitude, with magnitudes greater than 1.0 D. However, the population of CO_2 molecules about the open-metal sites is rather low. The primary sorption site afforded by WOFOUR-1-Ni is unique such that it induces high dipole magnitudes (close to 1.0 D) on the CO_2 molecules and it gives rise to a high occupancy of CO_2 molecules about this site.

Table S4: Partial charges (in units of electrons) for the chemically distinct atoms in CROFOUR-1-Ni, MOOFOUR-1-Ni, and WOFOUR-1-Ni. Numerical labeling of atoms corresponds to Figure S13.

Atom	Label	CROFOUR-1-Ni	MOOFOUR-1-Ni	WOFOUR-1-Ni
Ni	1	0.5290	0.2465	0.5517
Cr/Mo/W	2	1.2172	1.9315	1.9887
O	3	–0.6366	–0.7894	–0.9075
O	4	–0.6100	–0.7005	–0.8148
N	5	–0.1619	–0.2336	–0.3192
N	6	–0.2069	–0.2429	–0.2186
C	7	0.1488	0.2216	0.0966
C	8	0.1436	0.1700	0.1339
C	9	–0.4261	–0.4502	–0.3628
C	10	–0.4112	–0.4005	–0.3510
C	11	–0.2609	–0.2829	–0.2671
C	12	–0.2474	–0.2132	–0.2601
C	13	–0.4178	–0.3616	–0.3053
C	14	–0.4393	–0.4215	–0.3256
C	15	0.1875	0.1177	0.1209
C	16	0.1996	0.2141	0.0975
C	17	0.3659	0.3618	0.3682
C	18	0.3679	0.3262	0.3232
H	19	0.1240	0.1170	0.1520
H	20	0.1265	0.1259	0.1487
H	21	0.1685	0.1877	0.1729
H	22	0.1759	0.1775	0.1920
H	23	0.1924	0.2044	0.2050
H	24	0.1852	0.1844	0.2059
H	25	0.1730	0.1702	0.1714
H	26	0.1743	0.1729	0.1815
H	27	0.1017	0.1383	0.1483
H	28	0.1102	0.1176	0.1438

X-ray Crystallography

The X-ray diffraction data were collected using Bruker-AXS SMART-APEXII CCD diffractometer with a CuKα radiation (λ = 1.54178 Å). Indexing was performed using *APEX2*[36] (Difference Vectors method). Data integration and reduction were performed using SaintPlus 6.01.[37] Absorption correction was performed by multi-scan method implemented in SADABS.[38] Space groups were determined using XPREP implemented in APEX2.[36] The structure was solved using SHELXS-97 (direct methods) or using Apex2's Intrinsic Phasing and refined using

SHELXL-97 (full-matrix least-squares on F^2) contained in OLEX2[39]and WinGX v1.70.01[40-43]programs.

WOFOUR-1-Co: All non-hydrogen atoms were refined anisotropically. Hydrogen atoms of –CH groups were placed in geometrically calculated positions and included in the refinement process using riding model with isotropic thermal parameters: Uiso(H) = 1.2Ueq(-CH). Disordered solvent molecules have been refined as oxygen atoms (Water has been used during the synthesis).

WOFOUR-1-Ni: All non-hydrogen framework atoms were refined anisotropically. Hydrogen atoms of –CH groups were placed in geometrically calculated positions and included in the refinement process using riding model with isotropic thermal parameters: Uiso(H) = 1.2Ueq(-CH). Disordered solvent molecules have been refined as oxygen atoms. (Water has been used during the synthesis). One acetonitrile molecule is disordered over three positions. Crystal was a racemic twin: BASF = 0.579(7). Despite very low R factor (1.8%) some additional (very minor) twinning has been detected in diffraction pattern violating R centering. All attempts to include Obv/Rev twinning were unsuccessful. This does not seem to impact the structure quality significantly.

Table S4: Crystal data and structure refinement for **WOFOUR-1-Co** and **WOFOUR-1-Ni**.

Identification code	**WOFOUR-1-Co**	**WOFOUR-1-Ni**
Empirical formula	$C_{24}H_{20}CoN_4O_{9.08332}W$	$C_{25.33}H_{22}N_{4.67}NiO_{8.67}W$
Formula weight	752.55	773.04
Temperature/K	228.15	228(2)
Crystal system	trigonal	trigonal
Space group	R32	R32
a/Å	21.3175(8)	21.1295(3)
b/Å	21.3175(8)	21.1295(3)
c/Å	17.9653(9)	18.0194(3)
α/°	90.00	90.00
β/°	90.00	90.00
γ/°	120.00	120.00

Volume/Å^3	7070.3(5)	6967.06(18)
Z	9	9
ρ_{calc}mg/mm^3	1.591	1.658
m/mm^{-1}	11.243	7.982
F(000)	3291.0	3402.0
Crystal size/mm^3	0.21 × 0.06 × 0.05	0.21 × 0.14 × 0.1
2Θ range for data collection	6.86 to 136.44°	13.72 to 137.36°
Index ranges	$-24 \leq h \leq 25$, $-25 \leq k \leq 25$, $-21 \leq l \leq 21$	$-25 \leq h \leq 24$, $-25 \leq k \leq 25$, $-21 \leq l \leq 20$
Reflections collected	17407	15543
Independent reflections	2866[R(int) = 0.0748]	2841[R(int) = 0.0287]
Data/restraints/parameters	2866/0/212	2841/0/195
Goodness-of-fit on F^2	0.999	1.072
Final R indexes [I>=2σ (I)]	R_1 = 0.0271, wR_2 = 0.0617	R_1 = 0.0187, wR_2 = 0.0488
Final R indexes [all data]	R_1 = 0.0286, wR_2 = 0.0622	R_1 = 0.0188, wR_2 = 0.0488
Largest diff. peak/hole / e Å^{-3}	0.43/-1.01	0.60/-0.76
Flack parameter	0.074(8)	0.00(5)

Additional References:

1. D. Wu, J. J. Gassensmith, D. Gouvea, S. Ushakov, J. F. Stoddart and A. Navrotsky, *Journal of the American Chemical Society*, 2013, **135**, 6790-6793.
2. T. M. McDonald, D. M. D'Alessandro, R. Krishna and J. R. Long, *Chemical Science*, 2011, **2**, 2022.
3. A. Demessence, D. M. D'Alessandro, M. L. Foo and J. R. Long, *Journal of the American Chemical Society*, 2009, **131**, 8784-8786.
4. J. M. Gu, T. H. Kwon, J. H. Park and S. Huh, *Dalton Transactions*, 2010, **39**, 5608-5610.

5. T. M. McDonald, W. R. Lee, J. A. Mason, B. M. Wiers, C. S. Hong and J. R. Long, *Journal of the American Chemical Society*, 2012, **134**, 7056-7065.
6. P. L. Llewellyn, S. Bourrelly, C. Serre, A. Vimont, M. Daturi, L. Hamon, G. De Weireld, J.-S. Chang, D.-Y. Hong, Y. Kyu Hwang, S. HwaJhung and G. r. Férey, *Langmuir*, 2008, **24**, 7245-7250.
7. D. X. Xue, A. J. Cairns, Y. Belmabkhout, L. Wojtas, Y. Liu, M. H. Alkordi and M. Eddaoudi, *Journal of the American Chemical Society*, 2013, **135**, 7660-7667.
8. M. H. Mohamed, S. K. Elsaidi, L. Wojtas, T. Pham, K. A. Forrest, B. Tudor, B. Space and M. J. Zaworotko, *Journal of the American Chemical Society*, 2012, **134**, 19556-19559.
9. B. Arstad, H. Fjellvåg, K. Kongshaug, O. Swang and R. Blom, *Adsorption*, 2008, **14**, 755-762.
10. J. Kim, S.-T. Yang, S. B. Choi, J. Sim, J. Kim and W.-S. Ahn, *Journal of Materials Chemistry*, 2011, **21**, 3070-3076.
11. X. Si, C. Jiao, F. Li, J. Zhang, S. Wang, S. Liu, Z. Li, L. Sun, F. Xu, Z. Gabelica and C. Schick, *Energy & Environmental Science*, 2011, **4**, 4522-4527.
12. S. R. Caskey, A. G. Wong-Foy and A. J. Matzger, *Journal of the American Chemical Society*, 2008, **130**, 10870-10871.
13. J. An, S. J. Geib and N. L. Rosi, *Journal of the American Chemical Society*, 2009, **132**, 38-39.
14. S. S. Iremonger, J. Liang, R. Vaidhyanathan, I. Martens, G. K. Shimizu, T. D. Daff, M. Z. Aghaji, S. Yeganegi and T. K. Woo, *Journal of the American Chemical Society*, 2011, **133**, 20048-20051.
15. P. D. Dietzel, R. E. Johnsen, H. Fjellvag, S. Bordiga, E. Groppo, S. Chavan and R. Blom, *Chemical Communications*, 2008, 5125-5127.
16. R. Vaidhyanathan, S. S. Iremonger, K. W. Dawson and G. K. H. Shimizu, *Chemical Communications*, 2009, 5230.
17. J. A. R. Navarro, E. Barea, J. M. Salas, N. Masciocchi, S. Galli, A. Sironi, C. O. Ania and J. B. Parra, *Journal of Materials Chemistry*, 2007, **17**, 1939.
18. P. Nugent, Y. Belmabkhout, S. D. Burd, A. J. Cairns, R. Luebke, K. Forrest, T. Pham, S. Ma, B. Space, L. Wojtas, M. Eddaoudi and M. J. Zaworotko, *Nature*, 2013.
19. A. L. Myers and J. M. Prausnitz, *AIChE Journal*, 1965, **11**, 121-127.
20. R. T. Yang, *Gas Separation by Adsorption Processes*; Imperial College Press, 1986.
21. K. Sumida, D. L. Rogow, J. A. Mason, T. M. McDonald, E. D. Bloch, Z. R. Herm, T.-H. Bae and J. R. Long, *Chemical Reviews*, 2012, **112**, 724-781.
22. M. Valiev, E. Bylaska, N. Govind, K. Kowalski, T. Straatsma, H. V. Dam, D. Wang, J. Nieplocha, E. Apra, T. Windus and W. de Jong, *Comput. Phys. Commun.*, 2010, **181**, 1477−1489.
23. W. J. Stevens, H. Basch and M. Krauss, *J. Chem. Phys.*, 1984, **81**, 6026.
24. P. J. Hay and W. R. Wadt, *J. Chem. Phys.*, 1985, **82**, 270.
25. L. A. LaJohn, P. A. Christiansen, R. B. Ross, T. Atashroo and W. C. Ermler, *J. Chem. Phys.*, 1987, **87**, 2812.
26. L. E. Chirlian and M. M. Francl, *J. Comput. Chem.*, 1987, **8**, 894−905.
27. C. M. Breneman and K. B. Wiberg, *J. Comput. Chem.*, 1990, **11**, 361−373.
28. F. Nouar, J. F. Eubank, T. Bousquet, L. Wojtas, M. J. Zaworotko and M. Eddaoudi, *Journal of the American Chemical Society*, 2008, **130**, 1833-1835.
29. D. Zhao, D. Yuan, D. Sun and H.-C. Zhou, *Journal of the American Chemical Society*, 2009, **131**, 9186-9188.
30. D. Yuan, D. Zhao, D. Sun and H.-C. Zhou, *Angewandte Chemie International Edition*, 2010, **49**, 5357-5361.
31. B. Zheng, J. Bai, J. Duan, L. Wojtas and M. J. Zaworotko, *Journal of the American Chemical Society*, 2010, **133**, 748-751.
32. K. Uemura, A. Maeda, T. K. Maji, P. Kanoo and H. Kita, *European Journal of Inorganic Chemistry*, 2009, **2009**, 2329-2337.

33. K. A. Forrest, T. Pham, K. McLaughlin, J. L. Belof, A. C. Stern, M. J. Zaworotko and B. Space, *The Journal of Physical Chemistry C*, 2012, **116**, 15538-15549.
34. T. Pham, K. A. Forrest, K. McLaughlin, B. Tudor, P. Nugent, A. Hogan, A. Mullen, C. R. Cioce, M. J. Zaworotko and B. Space, *The Journal of Physical Chemistry C*, 2013, **117**, 9970-9982.
35. T. Pham, K. A. Forrest, P. Nugent, Y. Belmabkhout, R. Luebke, M. Eddaoudi, M. J. Zaworotko and B. Space, *The Journal of Physical Chemistry C*, 2013, **117**, 9340-9354.
36. Bruker (2008). *APEX2* (Version 2008.1-0). Bruker AXS Inc., Madison, Wisconsin, USA.
37. Bruker (2001b). SAINT-V6.28A. Data Reduction Software.
38. G. M. Sheldrick, (1996). *SADABS. Program for Empirical AbsorptionCorrection.* University of Gottingen, Germany.
39. O. V. Dolomanov, L. J. Bourhis, R. J. Gildea, J. A. K. Howard, H. Puschmann, , OLEX2: A complete structure solution, refinement and analysis program. *J. Appl. Cryst.*, 2009, **42**, 339-341.
40. L. J. Farrugia*Appl. Cryst.*, 1999, **32**, 837-838.
41. G. M. Sheldrick, (1997) SHELXL-97. Program for the Refinement of Crystal.
42. G. M. Sheldrick, *ActaCryst.*, 1990, **A46**, 467-473.
43. G. M. Sheldrick, *ActaCryst.*, 2008, **A64**, 112-122.